Experimental Investigation of a Solar Collector Integrated with a Pulsating Heat Pipe and a Compound Parabolic Concentrator

Rong Ji Xu[1, 2*], Xiao Hui Zhang[1], Rui Xiang Wang[1], Shu Hui Xu[1], Hua Sheng Wang[2]

[1] *Beijing Engineering Research Center of Sustainable Energy and Buildings, Beijing University of Civil Engineering and Architecture, Beijing, 100044, China*

[2] *School of Engineering and Materials Science, Queen Mary University of London, London, E1 4NS, UK*

Abstract: The paper reports an experimental investigation of a newly proposed solar collector that integrates a closed-end pulsating heat pipe (PHP) and a compound parabolic concentrator (CPC). The PHP is used as an absorber due to its simple structure and high heat transfer capacity. The CPC has a concentration ratio of 3.4 and can be readily manufactured by three-dimensional printing. The CPC can significantly increase the incident solar irradiation intensity to the PHP absorber and also reduce the heat loss due to the decrease in the area of the hot surface. A prototype of the solar collector has been built, consisting of a PHP absorber bent by 4 mm diameter copper tube, CPC arrayed by 10×2 CPC units with the collection area of 300×427.6 mm^2, a hot water tank and a glass cover. HFE7100 was utilized as the working fluid at a filling ratio of 40%. The operating characteristics and thermal efficiency of the solar collector were experimentally studied. The steady and periodic temperature fluctuations of the evaporation and condensation sections of the PHP absorber indicate that the absorber works well with a thermal resistance of about 0.26 ℃/W. It is also found that, as the main factor, the thermal performance of the collector decreases with increasing evaporation temperature. The collector apparently shows start-up, operational and shutdown stages at the starting and ending temperatures of 75 °C. When the direct normal irradiance is 800 W/m^2, the instantaneous thermal efficiency of the solar collector can reach up to 50%.

* **Corresponding author**: Rong Ji Xu, Email: xurongji@bucea.edu.cn

Keywords: Solar collector; Pulsating heat pipe; Compound parabolic concentrator; Solar intensity.

1 Introduction

Solar energy is one among the most abundant, inexpensive, environment-friendly energies that can potentially meet the world's growing energy demand. The efficient mean to utilize solar energy is to convert solar energy into heat stored in water by solar thermal collectors [1]. Evacuated tube collectors and flat-plate solar collectors are the most commonly and widely used stationary solar collectors [2]. High-efficient heat transfer absorber and solar radiation concentration are the main methods to improve the performance of the solar thermal collector. Pandey and Chaurasiya [3] presented an overview on the different techniques to enhance the efficiency of flat plate collectors. The application of nanofluids as heat transfer fluid can improve the thermal efficiency of the collectors. Verma et al [4]. experimentally investigated the effect of a wide variety of nanofluids on the performance of flat plate solar collector. The thermal efficiency was improved by 23.5% using multiwalled carbon nanotubes/water instead of water up to 72.5%. In vacuum tube collectors, the efficiency was improved by 71.8% up to 93.4% due to the improved thermal properties of single walled carbon nanotubes nanofluid [5]. The combination of heat pipe and evacuated tube is an efficient way of solar collector due to its high heat transfer capacity. However, the thermal resistance between the absorber face of the vacuumed tube and the heat pipe determined the efficiency of the collector. The desalination efficiency was improved from 21.7% to 65.2% by using oil as the added fluid to the space between heat pipe and evacuated tube collector in a new desalination system, a combination of heat pipe and parabolic trough collector [6].

Pulsating heat pipe (PHP), which was proposed by Akachi [7] in the early 1990s as a new member of heat pipe, is one of the highly efficient absorber with simple structure and low-cost. At a steady state working stage, a self-sustained thermal-driven oscillating flow inside the tube is achieved, leading to higher heat transfer rate. Different from a traditional heat pipe, the sensible heat of the working fluid plays a major role in heat transfer [8]. Furthermore, complicated two-phase heat transfer occurs at a capillary scale. Previous efforts have mainly been focused on

explaining the working principle of PHPs. Heat flux has a significant effect on the thermal performance of PHP[9]. There are three working states of PHP, start-up, steady state and dry-out as the heat input increases. There exists a threshold heat flux at which PHPs start to operate. The thermal resistance of the PHPs decreases as the heat flux increases at steady state [10]. The operational regimes, including the start-up and dry-out under different heat inputs, were discussed in detail [11]. Kim and Lee [12] experimentally investigated the effect of channel geometry on the operating limit of microchannel pulsating heat pipes. The results showed that the square microchannel PHP can offer approximately 70% higher maximum allowable heat flux than the circular microchannel PHP at the same hydraulic diameter. Asymmetric channels decreased the thermal resistance of PHP under certain heat inputs[13].

Over the last decades, an increasing attention has been paid to the applications of PHPs, especially in the field of space, electronic cooling, heat recovery and solar thermal applications. A PHP air-preheater was designed and tested in a dryer and played a role of energy recovery and dehumidification [14]. PHP was also applied in a wire-on-tube heat exchanger as an extended surface and the heat transfer rate of the heat exchanger increased under different conditions [15, 16]. An unlooped PHP has been developed and tested in an electronic thermal management field with hybrid vehicle applications and the PHP functioned with high reliability and reproducibility and without any failure during the start-up or working stage [17]. A simplified theoretical model of PHP employed as the condenser in a vapor compression refrigeration system has been developed. The performance of the system was improved [18]. PHP had also been used as heat sink of a high power LED street light [19] and defrosting plate [20].

In the field of solar energy collection, the use of PHP as the heat receiver has presented an efficient performance that is comparable to that of the traditional heat pipe receiver. PHPs possess the advantages of simple structure, low cost, and high efficiency. Rittidech and Wannapakne [21] built a PHP flat-plate solar collector in 2007. The collector was placed on a sheet of black zinc and had a collection area of 2.00×0.97 m^2. An efficiency of approximately 62% was achieved. Choi et al.

[22] investigated the effect of the working fluid filling ratio and the cooling water flow rate on the top heat loss and performance of a PHP flat-plate solar collector. The radiation intensity was realized by using a halogen lamp solar simulator. The effect of evaporator length on the efficiency of a PHP flat-plate solar collector has also been investigated [23] and a multilayer perceptron neural network was trained and used to predict the behavior of the solar collector [24]. The maximum predicted thermal efficiency of the collector is 61.4%. An extra-long PHP was designed, constructed, and installed in a thermosiphon solar water heater, and the operating characteristic was investigated. Several sets of PHPs were placed in glass tubes to create a solar collector, another form of PHP receiver [25, 26]. An efficiency of approximately 76% was achieved [25], and the heat loss was reduced by the addition of the glass tube.

The PHP exhibits a great potential for use as a heat collector because of its high heat transfer capacity. However, the heat flux of the evaporation section of PHP should be sufficiently high to meet the demand of its steady and high-efficient work, which has a significant effect on the thermal performance of PHP [9]. Several experimental studies of PHP with similar structure to the PHP collector are listed and compared in Table 1. We can find in the application of PHP as solar heat collector or absorber the heat flux of the evaporation section is much lower than those in the experimental studies, which can be increased to improve the thermal performance of PHP. To this end, a solar concentrator is necessary. Compound parabolic concentrator (CPC), which is frequently utilized in low-temperature applications as a concentrating non-imaging concentrator [27], is introduced to concentrate solar radiation to the PHP absorber. Therefor, a novel solar collector integrated with a PHP and a CPC is proposed. The introduction of CPC with a proper concentration ratio can increase the heat flux of the PHP absorber so that the efficient heat transfer capacity of PHP is fully utilized. In the new collector, solar energy is concentrated by CPC instead of the absorb plate of the plate solar collector. The heat loss of the new collector will be reduced by decreasing the hot surface area. From another point of view, the disadvantage of CPC is the size, which depends on the size of the absorber, affecting the combination of the CPC collector and buildings.

104 The diameter of PHP is usually not more than 4mm that is much smaller than the traditional heat
105 pipe absorber. When PHP is used as absorber, the size of CPC can be the same as that of the plate
106 solar collector. This makes it easy to combine the new collector to buildings.

107 In this work, the detailed design of the collector is presented. The operating characteristics and
108 thermal performance of the collector are tested under different weather conditions, and the features
109 of the collector are also discussed.

110 Table 1 Summary of dimensions, working fluid and heat flux of PHPs in literature

Authors	Parameters of evaporation section				Q (W)	q_{rad} (W/cm^2)	Working fluid	Solar collector
	ID(mm)	OD(mm)	n	A_{rad}(cm^2)				
Rittidech et al. [21]	3	4	14	7033.60	300~900	0.082~0.248	R-134a	Y
Rittidech et al. [25]	3	4	20	7536	600~1350	0.046~0.115	R-134a	Y
Yang et al. [26]	3	5	12	3015.93	20~90 50~350	0.0067~0.030 0.017~0.117	water	Y
Nguyen et al. [22]	2	4	8	492.35	66.766 79.013 87.955 101.063	0.1356 0.1605 0.1786 0.2053		Y
Kargarsharifabad et al. [23]	2	4	21	10857 8218 5579	860~1440 645~1080 430~720	0.092~0.133 0.079~0.131 0.077~0.129	water	Y
Yoon et al. [28]	2	3.2	19	267.28	100~600	0.374~2.245	water	N
Zhang et al. [29]	1.18	2	3	20.99	8~30 10~30 20~50	0.381~1.429 0.476~1.429 0.953~2.382	FC72 ethanol water	N
Borgmeyer et al. [30]	1.59	2.69*	28	46.78	50~160	1.069~3.420	water ethanol flutec PP2	N
Dmitrin et al. [31]	2	4*	8	180.86	30~100	0.166~0.553	water	N
Yang et al. [32]	1 2	2 3	40	12.38 22.79	50~380	4.038~30.687 2.194~16.675	R123	N
Sarangi et al. [33]	1	2	16	200.96	20~56 12.5~96	0.10~0.28 0.062~0.478	water ethanol	N
Naik et al. [34]	1.95	3	1	17.44	9~15	0.516~0.860	acetone methanol ethanol	N
Mameli et al. [35]	2	4	2	15.42	0~30 40~100	1.945 2.593~6.484	ethanol	N
Cui et al. [36]	2	4	5	285.36	5~15	0.018~0.053	water	N

					20 35~50 65~100	0.07 0.122~0.175 0.228~0.350	methanol ethanol acetone	
Karthikeyan et al. [37]	2.3	3.3	5	41.47	50~180 50~240 50~240	1.206~4.341 1.206~5.875 1.206~5.875	water Ag colloidal Cu nanofluids	N
Hao et al. [38]	2	4*	4 6	13.44 20.16	30~105 30~280	2.232~7.813 1.488~13.889	water	N
Mohammadi et al. [39]	2.2	3.2	4	65.95	25~85	0.379~1.289	water	N
Karthikeyan et al. [40]	2	3	8	90.48	30~500	0.332~5.526	water	N
Tseng et al. [41]	2.4	3	4	72.38	20~140	0.276~1.934	water methanol HFE-7100	N
Mohammadi et al. [42]	1.75	3	5	74.85	20~140	0.267~1.870	water nanofluid	N
Mameli et al. [43]	1.1	2	16	15.51	10~100	0.645~6.449	FC-72	N
Xian [44]	2	6	5	118.20	40~110	0.338~0.931	water	N
Pachghare et al. [45]	2	3.6	2	21.57	8~80	0.371~3.709	water ethanol methanol	N
Xian et al. [46]	2	6	5	118.20	30~40 40~100 100~110	0.254~0.338 0.338~0.846 0.846~0.931	water	N

* The thickness of the tube was not given and is taken to be 0.5 mm here.

2 Design of the PHP solar collector with CPC

2.1 Solar collector and PHP absorber

Figure 1 shows the configuration and dimensions of the solar collector which consists of a PHP absorber, CPC, a hot water tank and a glass cover. The PHP absorber is made of copper tubes having an outer diameter of 4 mm and an inside diameter of 2 mm. The bending radius depends on the capture width of the CPC (see section below). The evaporation section is 300 mm long and is painted black with absorption rate of 0.85. The evaporation section of the PHP absorber is fixed at the focus of the CPC and the outer diameter of the absorber is the original cycle of the CPC so that all solar radiation can be reflected to the PHP. The condensation section is 200 mm long and is sealed inside the hot water tank. The hot water tank is made of stainless steel plate with dimensions

of 500 mm × 250 mm × 25 mm and 1 mm wall thickness. The outer surface is insulated by polyurethane. No adiabatic section exists between the evaporator and condenser sections. The PHP absorber, CPC, and hot water tank are fixed on a wood plate. The solar collector is insulated by polymethyl methacrylate to minimize heat loss to ambient.

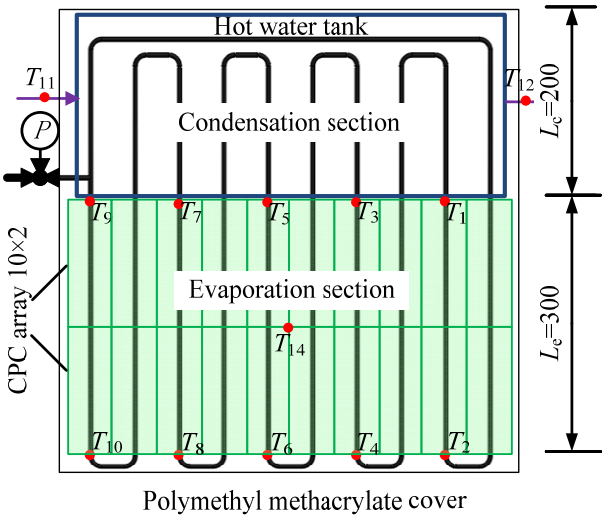

(a)

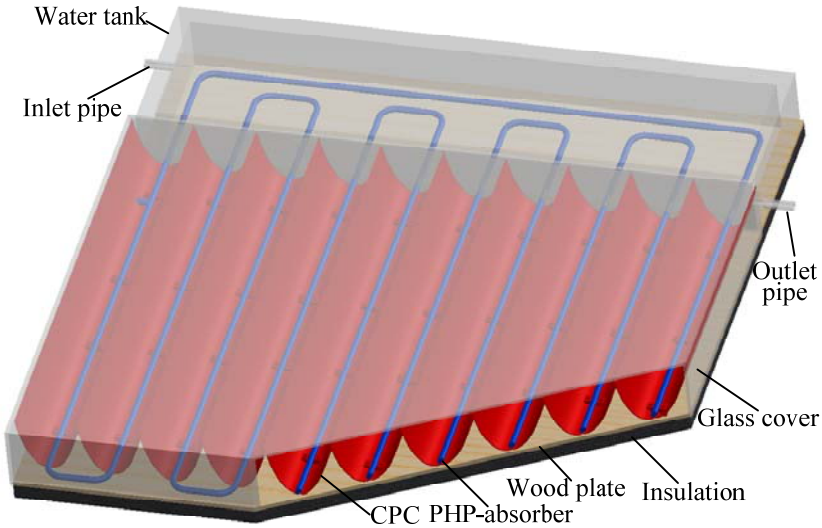

(b)

Fig. 1. Schematic of solar collector integrated with CPC and PHP. (a) top view; (b) model

2.2 Design of the CPC

CPC is introduced to increase the solar irradiation intensity to the PHP absorber and hence its heat flux. The CPC consists of two parabolas with compound rotation, and most of the beam and

diffuse radiation can be collected and reflected on the absorber surface without a complicated solar tracking system (see Fig. 2).

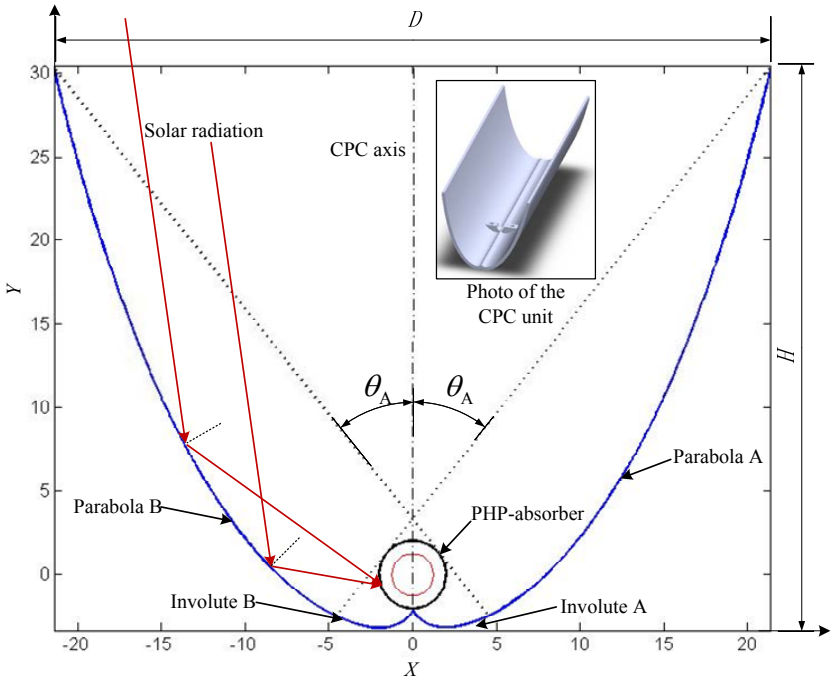

Fig. 2. Geometry and dimension of CPC and PHP absorber and coordinator

The CPC involute is defined by Eq. (1) as

$$\begin{cases} X = \dfrac{d}{2}\left(\sin\varphi - \varphi\cos\varphi\right) \\ Y = -\dfrac{d}{2}\left(\varphi\sin\varphi + \cos\varphi\right) \end{cases}. \tag{1}$$

for $0 \le \varphi \le 90^\circ + \theta_A$.

The parabola line is defined by Eq. (2) as

$$\begin{cases} X = \dfrac{d}{2}\left(\sin\varphi - A^* \cos\varphi\right) \\ Y = -\dfrac{d}{2}\left(A^* \sin\varphi + \cos\varphi\right) \end{cases} \tag{2}$$

for $90^\circ + \theta_A \le \varphi \le 270^\circ + \theta_A$

where

$$A^* = \frac{\dfrac{\pi}{2} + \theta_A + \varphi - \cos\left(\varphi - \theta_A\right)}{1 + \sin\left(\varphi - \theta_A\right)}, \tag{3}$$

φ is the angle between the incident ray and the X-axis. θ_A is the aperture angle of the CPC given

by Eq. (4)

$$\theta_A = \arcsin(\frac{1}{CR}) \quad . \tag{4}$$

The concentration ratio (*CR*) is defined by Eq. (5) as

$$CR = \frac{D}{\pi \times d} \quad , \tag{5}$$

where *D* is the aperture width and *d* is the outer diameter of the PHP absorber. The average heat flux of evaporation section of the PHP absorber can be calculated by Eq. (6)

$$q = \frac{D \times I}{\pi \times d} = CR \times I \, . \tag{6}$$

where *I* is the solar irradiation intensity measured using a pyranometer.

Two key aspects are considered in the design of the CPC. One is to ensure the existence of sufficient heat flux of the evaporation section of the PHP, and the other is to check that the ratio of height to width is not too large. The geometric shape of the CPC depends on the outer diameter of the PHP absorber, and the size of the CPC depends on the concentration ratio *CR* or opening width *D*. In the present work, the outer diameter of the PHP absorber is 4 mm. According to the values of heat flux in literature [36, 40, 42, 44, 46] which is 0.166W/cm^2~5.526 W/cm^2, a preliminary *CR* = 5 was selected, and the interception ratio of the CPC is 4/5. Thus, the actual *CR* is 3.40 and the aperture width *D* is 42.76 mm. The newly designed solar collector can reach an average heat flux of 0.17~0.34 W/cm^2 under the solar irradiation density of 500~1000 W/m^2. This level of heat flux ensures that the PHP can work steadily as in literature [36, 40, 42, 44, 46]. The introduction of CPC to the PHP solar collector is thus reasonable and necessary.

Once the CPC size was finally determined, the model line was drawn using Eqs. (1) to (5) in Malab and then exported into Solidworks to build a 3D model. To attach a reflective sheet with 0.1 mm thickness onto the inner surface of the CPC, the inner surface was cut off by 0.1 mm depth. A fastener was designed to fix the pipe of the PHP. The CPC was manufactured using a three-dimensional printer with an accuracy of 0.02 mm. The limitation of the three-dimensional

printer in terms of size required the utilization of CPC units to assemble the entire CPC (see Fig. 2). The length of one CPC unit is 150 mm. Two units are lined for one pipe of the PHP evaporation section, and 10 × 2 array CPC units are arranged for the entire PHP absorber. The total area of the CPC is 0.12828 m^2 for solar energy collection. The aluminum reflective sheet with a reflective ratio of 0.80–0.90 was attached to the inside surface of the CPC.

3 Experimental setup and procedures

3.1 Experimental setup

Figure 3 shows the apparatus which consists of the solar PHP absorber, a hot water loop and data acquisition system. The hot water loop was built to maintain a proper heat-collecting temperature of the solar collector. The hot water loop includes a hot water tank, pump, fin-tube heat exchanger and flow meter. The pump drives the circulation of the hot water. The hot water is cooled in the air-cooled heat exchanger, then circulated back to the hot water tank through the flow meter with a reduced temperature and finally heated through the condensation section.

Figure 3 also shows the data acquisition system and the temperatures, total solar radiation intensity, and flow rate of the hot water are measured. Ten T-type thermocouples (Omega®, bead dimension of 0.8 mm, accuracy ±0.1 K after calibration), numbered T_1 to T_{10}, were soldered on the external tube wall of the PHP absorber (see Fig.1). The PHP absorber has five turns and two thermocouples are used for each turn. One thermocouple is located at the beginning of the evaporation section and another thermocouple is located at the end where the condensation section begins. Two thermocouples, T_{11} and T_{12}, were used to measure the hot water temperatures at the inlet and outlet of the hot water tank. The air temperature inside the cover at the center of the evaporation section of the PHP absorber was also measured using thermocouple T_{14} and for the ambient air temperature was measured by thermocouple T_{13}. A data logger (Agilent34972A Data Acquisition/Switch Unit, with ±1 K accuracy) was utilized to record the temperatures. Solar radiation intensity was measured and recorded using a solar pyranometer (TES-1333R) with an

accuracy of ±10 W/m^2. The frequency of the temperature and solar intensity data acquisition is 0.5 Hz. A rotameter (Senlod, LZB-6) with an accuracy of 2.5% at a 60 L/ H flow range was utilized to measure the flow rate of the hot water.

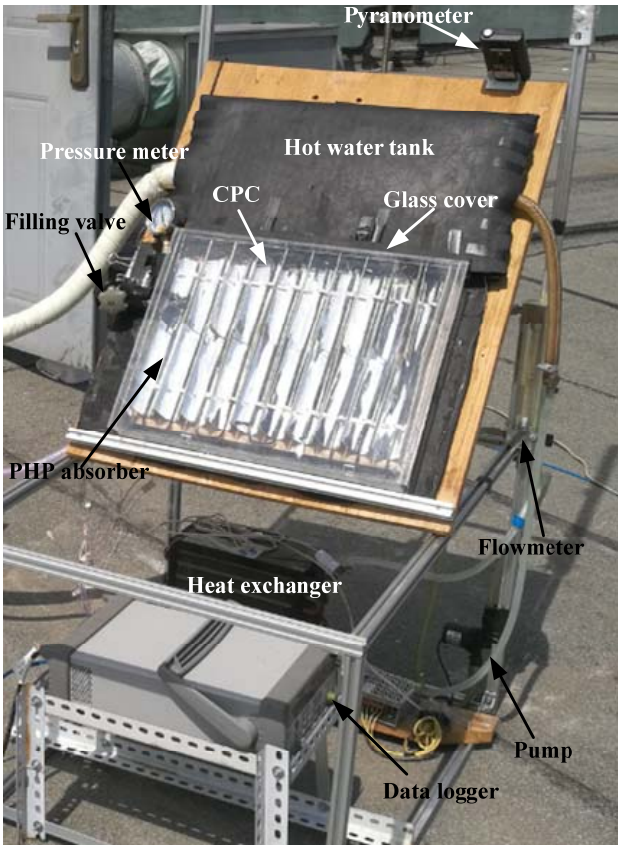

(a)

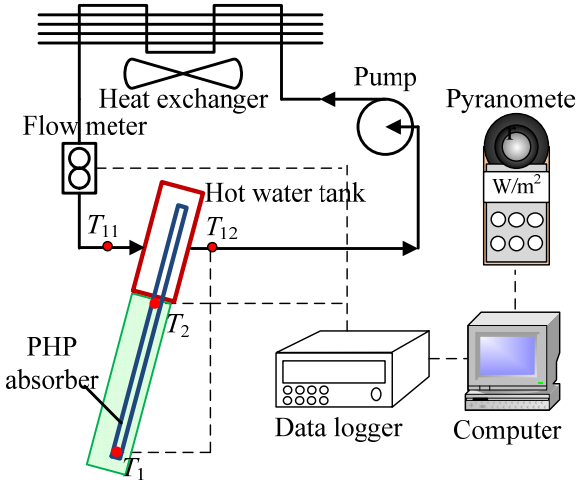

(b)

Fig. 3. Experimental set up. (a) Photograph; (b) Schematic and data acquisition

3.2 Experimental conditions and procedure

All experiments were conducted on the top of a building in Beijing, China (latitude: 39°48′; longitude: 116°28′). The daily experiment time was between 9:00 AM and 5:00 PM because approximately 90% of solar energy is obtained in this period of time. The experiments were conducted from May 14, 2015 to September 5, 2015.

In the present work, a pressure of 0.1 Pa in the tube can be created using a double-stage rotary vacuum pump and can be maintained for 24 h without increasing. HFC7100 (C4F9OCH3) was filled at a volume filling ratio of 40%. The inclination angle of the solar collector was adjusted to 45°. The flow rate of the hot water was fixed to 50 L/h, and the pump of the hot water loop was not turned on until the temperature of the hot water reached 40 °C that was maintained.

3.3 Data processing

The temperature fluctuation is another key parameter indicating the operating characteristic of the solar collector. Apart from the temperature fluctuation, the average temperatures of the evaporation (T_e) and condensation (T_c) sections are also considered.

The thermal resistance of the PHP absorber is determined by

$$R_T = (T_e - T_c) / Q_s = (T_e - T_c) / (IA). \quad (7)$$

The instantaneous quantity of heat transferred to water can be calculated by the flow rate, specific heat and temperature rise between the outlet and inlet of water.

$$Q_w = c_w m_w (T_{out} - T_{in}) \quad (8)$$

The instantaneous heat collecting efficiency of the solar collector is defined as the ratio of the heat absorbed by water to the total solar irradiation reached to the solar collector.

$$\eta = Q_w / Q_s = c_w m_w (T_{out} - T_{in}) / (IA), \quad (9)$$

where A is the area of the CPC array.

3.4 Uncertainty analysis

The maximum uncertainty of temperature is estimated to be ±1.1 K depending on the accuracy of the twelve T-type thermocouples ±0.1 K and the accuracy of the data logger ±1.0 K. The uncertainties of the water flow rate and solar irradiation intensity are 2.5% of the measuring range (±1.5L/h) and ±10 W/m^2, respectively. The uncertainties of thermal resistance of the PHP-absorber and thermal efficiency of the solar collector are obtained from Eqs. (7) and (9) using Eq. (10) [47].

$$w_R = \sqrt{\sum \left(\frac{\partial R}{\partial x_i} w_i \right)^2} \tag{10}$$

where w_R is the uncertainty of the dependent variable and w_i are the uncertainties of the independent variables. A summary of the maximum uncertainties of the main parameters are given in Table 2.

Table 2. Uncertainties of the measurements

Quantity	Max uncertainty
Temperature (K)	±1.1
Water flow rate	2.50%
Solar irradiation intensity (W/m^2)	±10
Temperatures of evaporation and condensation, (K)	0.64%
Thermal resistance	5.34%
Thermal efficiency	11.01%

4 Results and discussion

4.1 Operating characteristics of the PHP absorber

In present work, three representative tests were chosen to analyze the system performance. The first test was conducted on June 12, 2015 named as case I; the second test on June 13, 2015 named

as case II; and the third test on June 14, 2015 named as case III. The variations of the solar intensity during tests on the first two days were similar; whereas that on the third day was different.

Evaluation of the pulsating working condition was the first step in the experiments. Two indicators were adopted to verify whether or not the copper tube functions as a pulsating heat pipe or not. One indicator is the temperature fluctuation in the evaporation and adiabatic sections, and the other is the temperature increase in the evaporation section. If the PHP absorber does not work as a PHP or if dry-out occurs, the temperature of evaporator section will increase rapidly. In other words, if the temperature of the evaporation section does not increase along with the increase in solar intensity, the copper tube functions as PHP even without a pulsating temperature. These conditions are a guide to determine whether or not dry-out occurs, particularly under high solar intensity conditions. The same approach was used in Nguyen et al. [22].

Figure 4 shows the variations of the measured solar intensity and temperature (T_4 and T_5) of the PHP solar collector with local time for case I (a) and case II (b). It can be seen that the temperature fluctuation for case I and case II are similar under the similar solar intensity. The pulsating temperature pertains to the pulsation of vapor bubbles or liquid slug inside the tube as a result of different temperatures they have. For the PHP-absorber, there exists a minimum heat flux that starts up the pulsating flow [10]. Therefore, the operation of the solar collector appears three working stages, namely, start-up, steady state, and shutdown corresponding to the level of solar intensity. At the start-up stage, the temperature of the PHP increases rapidly as the solar intensity increases. It was observed that vapor bubbles does not generate in all of the tubes at the same time and instead generating small vapor bubbles in one or two tubes at 65 °C. The bubbles can reach the condensation section and the temperature exhibits a small fluctuation. When the temperature of the evaporation section reaches 75 °C, a sharp drop and fluctuation in temperature occur with no further increase. This marks the startup of the pulsating heat pipe. The startup time of the solar collector is approximately 11:00 AM, with a solar irradiation intensity of 750 W/m^2. In the next working stage, the temperature variation in the evaporation and condensation sections are violent and nearly

periodic. At this stage, the solar irradiation intensity reaches its highest value of the day and stable. With irradiation intensity decreases, the PHP enters the shutdown stage. As the solar irradiation intensity decreases, both the temperature fluctuation frequency and amplitude decrease until they disappear. The temperature declines rapidly, especially in the evaporation section. The ending time of the PHP absorber is approximately 2:00 PM, and the ending temperature of the evaporation section is about 75 °C (similar to startup). The first rapid drop in temperature was observed at the start-up stage because of the opening of the glass cover to check the thermocouples.

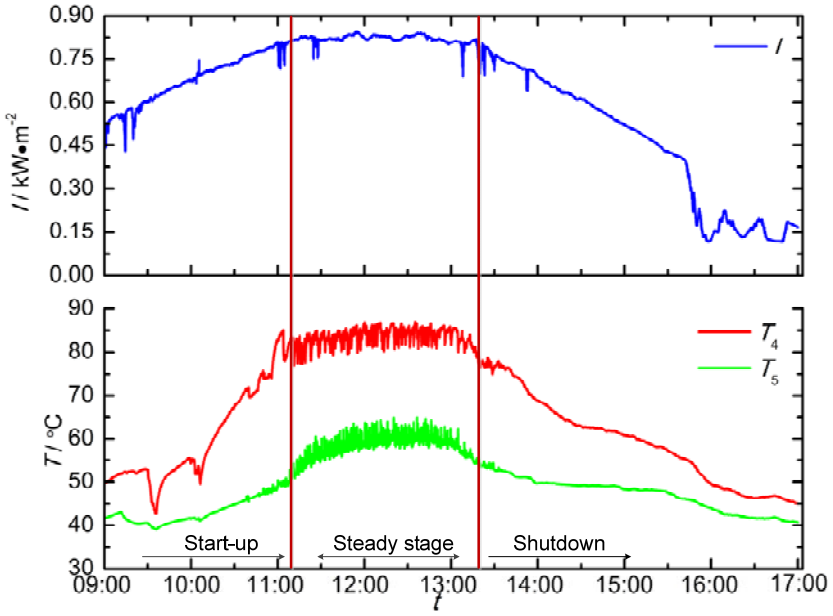

(a)

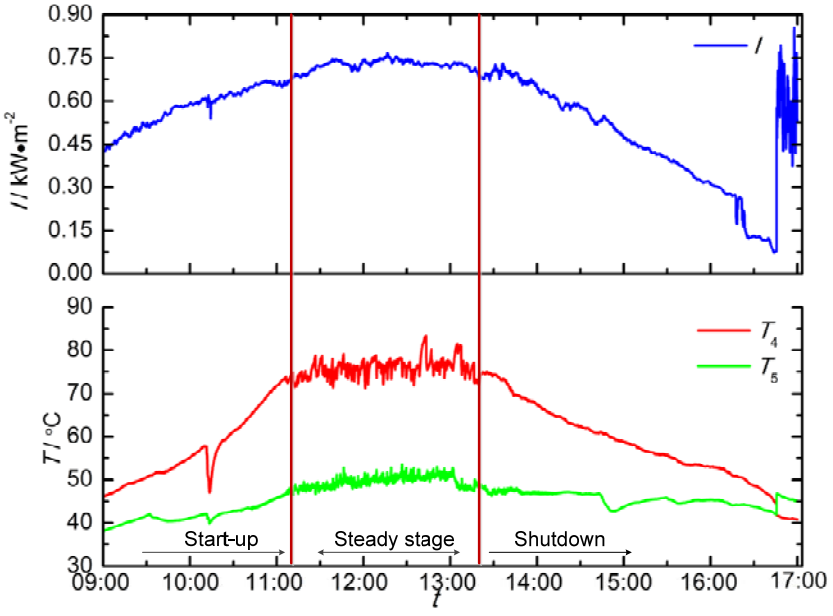

(b)

Fig. 4. Variations of solar intensity and measured temperatures at locations in solar collector (see Fig. 1 (a)) with local time for (a) Case I and (b) Case II.

The temperature fluctuations of the evaporation and condensation sections at the steady stage are steady and periodic. The temperature of evaporation and condensation sections are differences (approximately 30 K). The evaporating temperature is around 85 °C and the condensing temperature is approximately 55 °C for case I. This temperature difference is slightly larger than that in Case II because the solar irradiation intensity in Case I is higher. Both evaporation and condensation temperatures at the steady stage slightly decrease.

Figure 5 shows the variations of the thermal resistance in the PHP solar absorber at the steady working stage for Case I and Case II. The thermal resistance in Case I is steady and fluctuates between 0.26 °C/W and 0.29 °C/W. The working state of the PHP absorber is steady under a good working condition. The thermal resistance value is more reasonable than those found in literature [36, 40]. The design of the solar collector with PHP and CPC is thus reasonable.

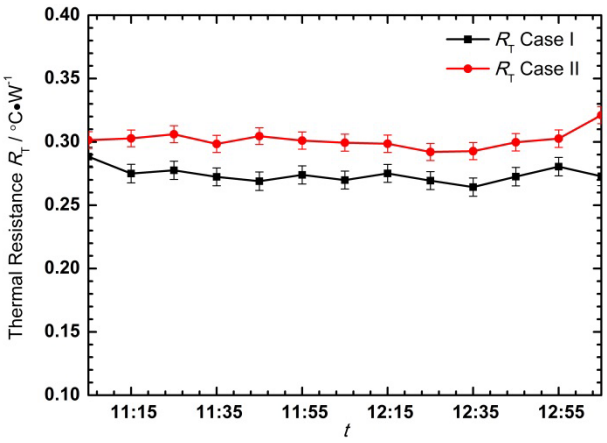

Fig. 5. Variations of thermal resistance of solar absorber at the steady working stage for Case I and Case II

To compare with the working characteristics of the PHP solar thermal collector, the temperature variation and thermal performance of the solar collector were tested on different days with different levels of solar irradiation intensity. Three working stages also exist for different solar irradiation intensities even on a cloudy day (see Fig. 6). The solar collector can still operate normally even under cloudy weather. The startup temperature is almost the same (approximately

75 °C) on different days. However, the temperature fluctuation appears larger and varies with the solar irradiation on cloudy days. The steady working stage is seen to be short, with a lower evaporation section temperature of approximately 70 °C and condensation section temperature of approximately 50 °C. The amplitude of temperature pulsation caused by the moving of liquid and bubble slugs in side PHP is significantly small.

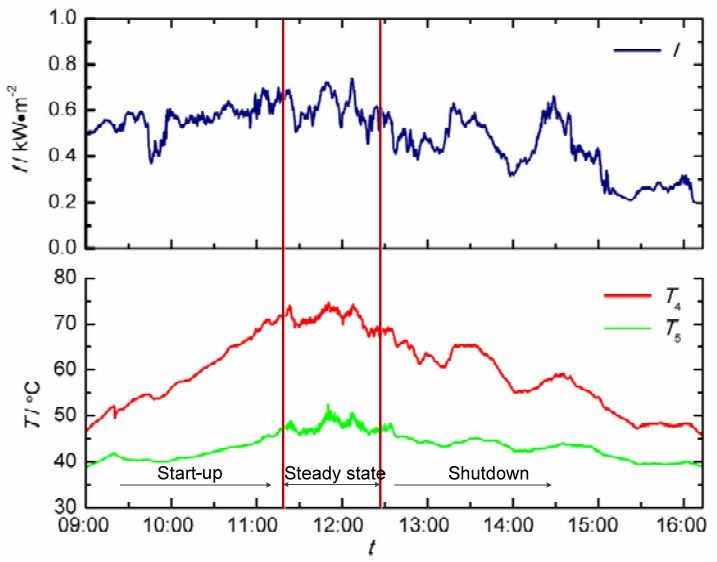

Fig. 6. Variations of solar intensity and measured temperatures at locations in solar collector (see Fig. 1 (a)) with local time for Case III.

Thermal resistance is an important indicator of the operation and performance of solar collectors. To further investigate the thermal resistance variation and influencing factors, the thermal resistance was statistically analyzed based on these three-day experimental data at steady state stage.

Figure 7 (a) shows the effect of solar irradiation intensity on the thermal resistance of the solar collector. The thermal resistance of the PHP absorber decreases with the increase in heat input, similar to traditional PHPs. The difference between traditional PHPs and the PHP absorber is in the heat flux distribution in the evaporation section. The heat flux distribution of the PHP absorber is uneven due to the reflection of solar radiation of the CPC. The thermal resistance decreases from 0.37 °C/W to 0.25 °C/W with the increase in solar irradiation intensity from 500 W/m^2 to 900 W/m^2.

The results demonstrate that the PHP absorber can work well at a proper heat flux under solar radiation intensity. Figure 7 (b) and (c) show the influence of ambient and evaporation temperatures on the thermal resistance of the PHP absorber. The thermal resistance decreases with the increase in ambient temperature. The ambient temperature is the main factor that influences the heat loss of the solar collector. When the ambient temperature increases, the heat loss decreases leading more heat transferred by the PHP absorber to the condensation section. It can be seen that the thermal resistance of the PHP absorber decreases with the increase in evaporation temperature. This result is encouraging because it shows that the combination of CPC and PHP can be effectively utilized in high-temperature solar thermal collectors.

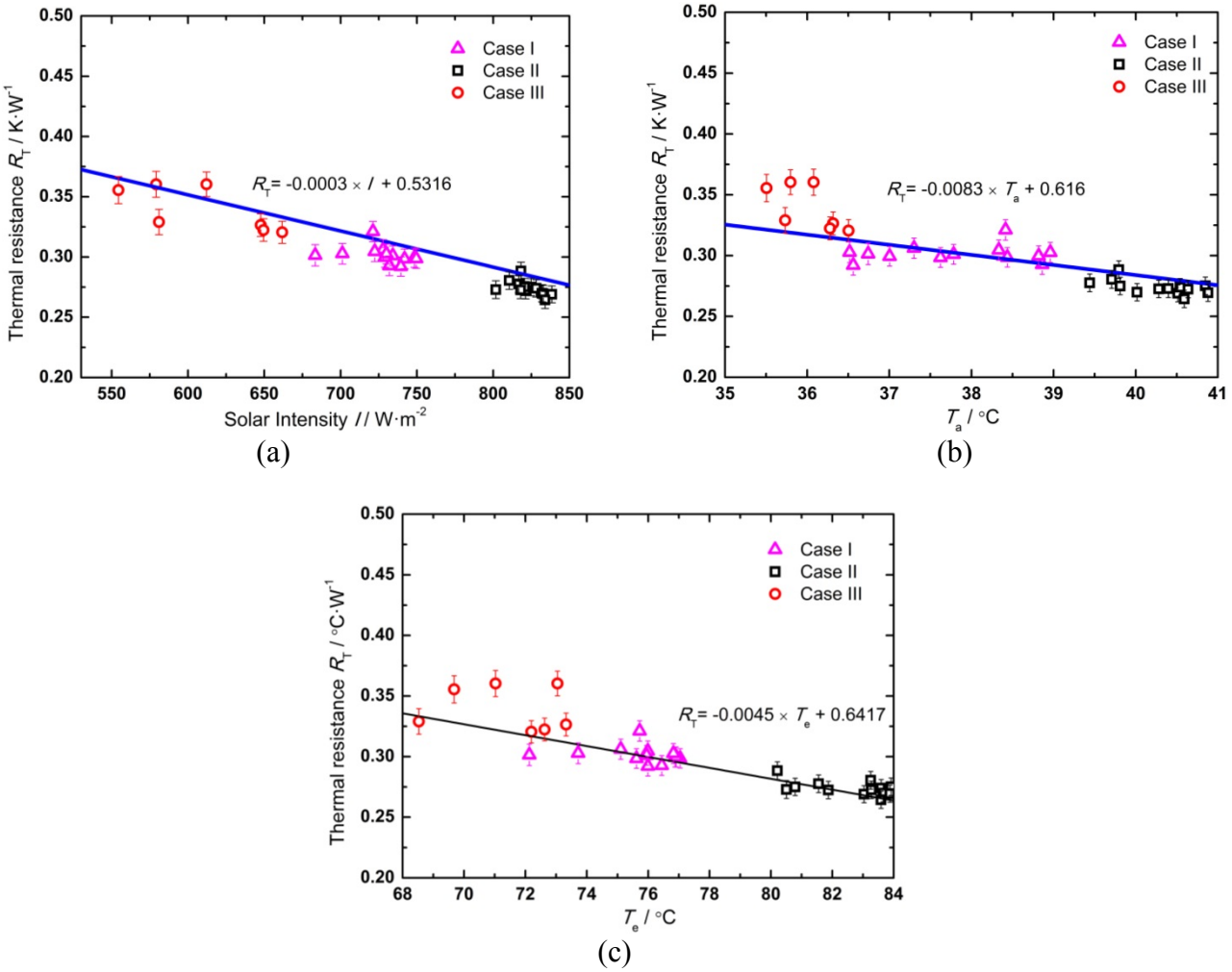

Fig. 7. Effects on thermal resistance of PHP absorber. (a) solar intensity; (b) ambient temperature; (c) evaporation temperature

4.2 Thermal efficiency of the solar collector

The the performance of the solar collector at the steady working stage is shown in Fig. 8. The instantaneous heat collecting efficiency is stable. The efficiencies are approximately 50% with a solar intensity of 800 W/m^2, and 40% with a solar intensity of 730 W/m^2. Respectively the value of efficiency is comparable to those in literature [36, 40, 43]. The performance of the solar collector on a cloudy day is shown in Fig. 8. It can be found that the fluctuation of instantaneous efficiency of the collector on a cloudy day is larger but it still achieves an overall efficiency of approximately 50%. Although large fluctuations in solar irradiation occur, the collector can still work and achieve highly satisfactory collection efficiency, thereby indicating the reliability of its operation. Furthermore, the thermal performance of the collector can be improved by increasing the reflective ratio of the reflective film and absorption coating efficiency and reducing the heat loss of the glass cover.

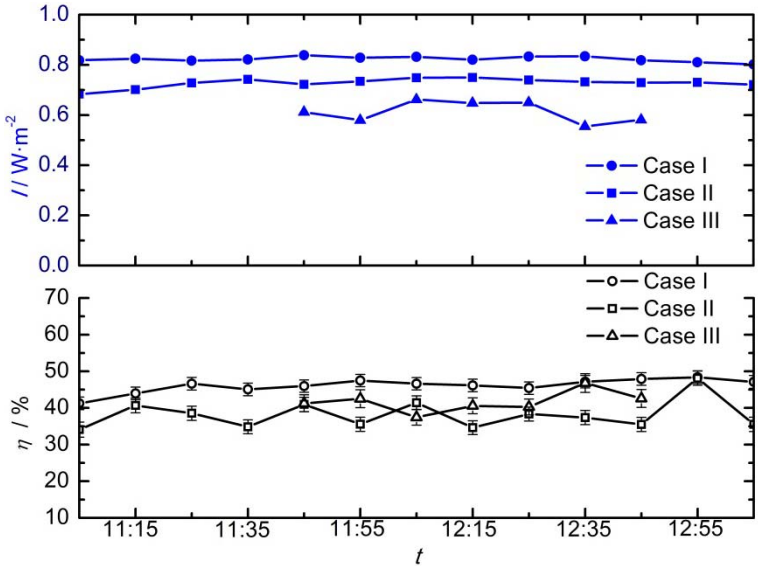

Fig. 8. Variations of thermal efficiency of solar collector with local time

The main factors that influence the thermal performance of the collector include solar intensity, ambient temperature, evaporation temperature, and thermal resistance of the PHP absorber. To investigate the tendencies among them, several results were analyzed. Figure 9 (a) shows the effect of solar intensity on the thermal performance of the collector. The thermal performance of the collector depends on solar intensity. The efficiency increases with the increase in solar intensity;

however, the rate of the increase is extremely low. The thermal performance of the PHP absorber is steady for the entire range of the solar intensity. This finding means that the collector has good stability. The same condition can be found in Fig. 9 (b), which shows the effect of ambient temperature on the thermal performance of the collector. The ambient temperature is the main parameter for the heat loss of the collector. Figure 9 (c) shows that the efficiency of the collector increases with the increase in evaporation temperature because the thermal resistance of the PHP absorber is lower at a higher evaporation temperature. Furthermore, the water tank obtains additional heat from the PHP absorber. Conversely, the heat loss of the collector is high when the evaporation temperature is high. In consideration of the solar energy input, heat loss, and heat collection, the thermal performance of the collector increases with the increase in evaporation temperature and the decrease in the thermal resistance of the PHP absorber is the main factor that influences its thermal performance, as shown in Fig. 9 (d).

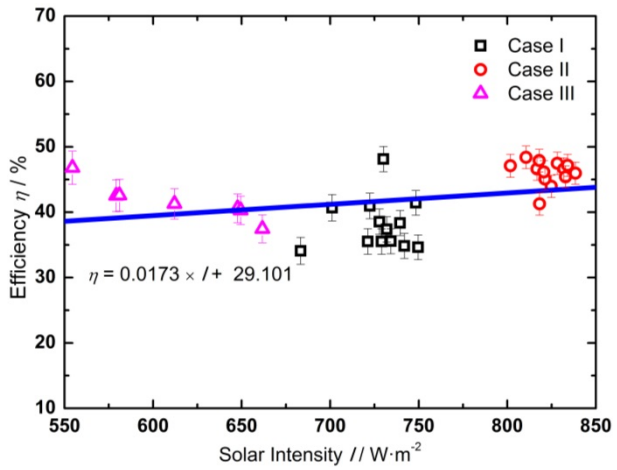

(a)

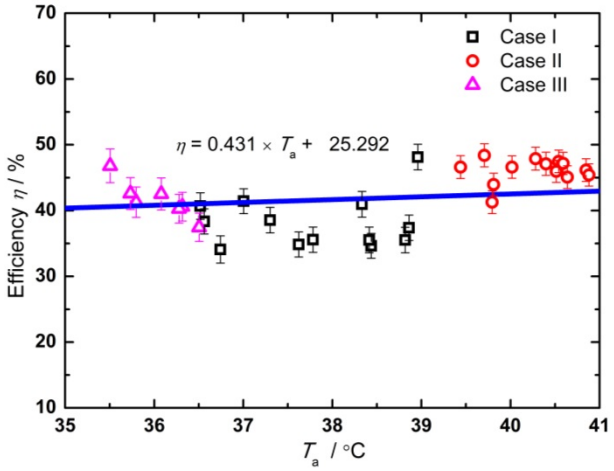

(b)

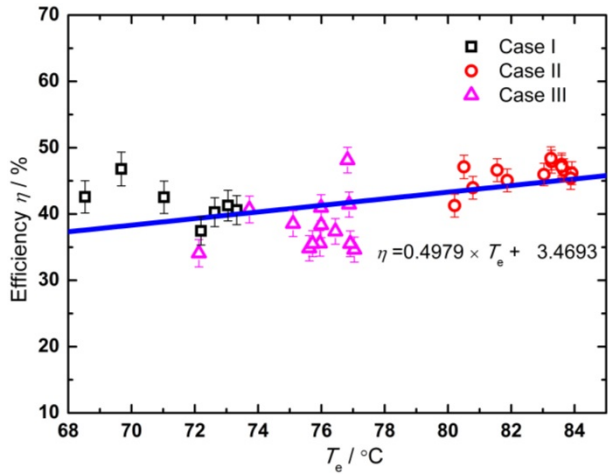

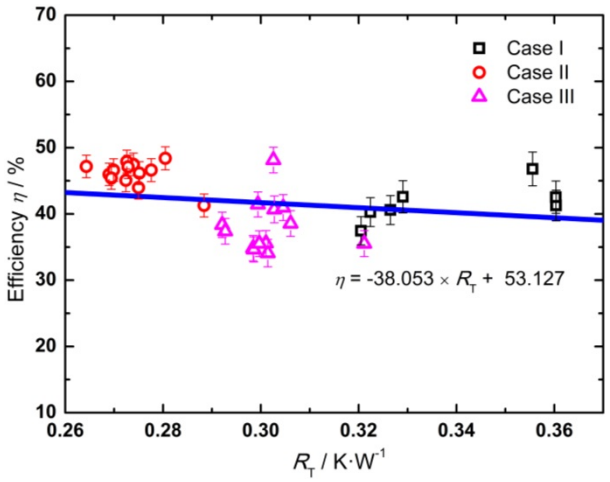

(c) (d)

Fig. 9. Effects on thermal efficiency of solar collector. (a) solar intensity; (b) ambient temperature; (c) evaporation temperature; (d) thermal resistance of the PHP absorber

Figure 10 shows the effect of the $(T_p\text{-}T_a)/I$ on the thermal efficiency of the collector. The present results are compared with the performance curves of the solar collectors by heat pipe systems [37] and pulsating heat pipe system [25]. The $(T_p\text{-}T_a)/I$ values of the present work are higher than those in literatures [25] and [37] due to the solar concentration by CPC. The thermal efficiency of the present work is slightly lower. The main reason is that no seal exists between the glass cover and the wood board and also the distance from the glass cover to the wood board. The thermal efficiency of the new collector increase with the increases of $(T_p\text{-}T_a)/I$ and the trend is different from those in literatures [25] and [48]. The reason is that the thermal resistance of the PHP-absorber, which is the main factor influencing the thermal efficiency of the collector, decreases with the increase in solar irradiation intensity and evaporation temperature (see Fig.7(c)).

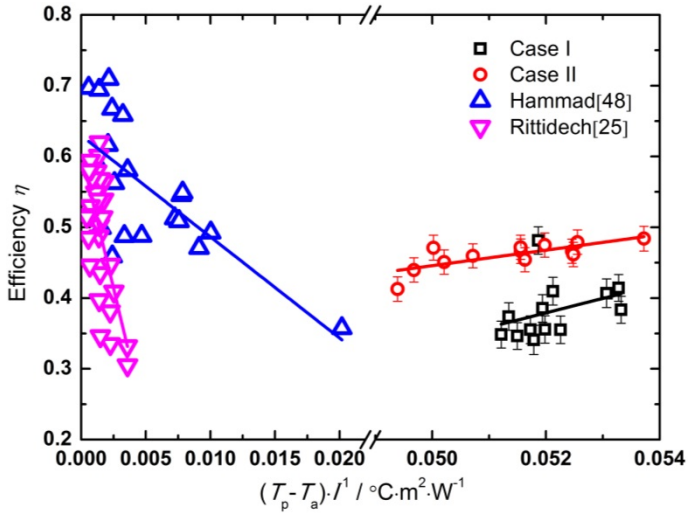

Fig. 10. Effect of the $(T_p\text{-}T_a)/I$ on the collector efficiency, $T_p=(T_e+T_c)/2$

4.3 Discussion on the new solar collector with PHP and CPC

To match the heat transfer capacity of the PHP absorber and solar irradiation intensity, a solar collector equipped with PHP and CPC has been developed. The evaporation section of the PHP absorber receives proper heat flux that works steadily due to the introduction of CPC. Furthermore,

the heat loss to the surrounding air was decreased by reducing the hot surface area of the collector. From the perspective of the collector of CPC, PHP is a good choice for its small endothermic radius. In the present work, the total thickness of the collector is less than 50 mm with the CPC at a concentration ratio of 3.4. Additionally, the new collector also has the advantage of protection from freezing, which is suitable to the application of low freezing point working fluid. Generally, it presents a new efficient method of solar thermal collecting at centimeter scale and has great potential in many applications.

The design of the proposed solar collector still has a drawback of short steady working hours. The CPC aperture angle causes the late startup and the early shutdown. Fortunately, gravity has minimal effect on the thermal performance of the PHP [9]. The working hours of the collector can be prolonged by changing the direction of CPC from vertical to horizontal in order to receive more solar energy and to work for the entire day.

5 Conclusions

A novel solar collector that integrates a closed-end PHP and a CPC has been proposed, built and tested. The effects of operating parameters on the operating characteristics of the PHP absorber and the thermal performance of the solar collector were investigated under different weather conditions. The following conclusions can be drawn.

1) The collector apparently shows start-up, operational and shutdown stages at the starting and ending temperatures of 75 °C. The solar collector can stably operate even in cloudy days.
2) The thermal resistance of the PHP absorber decreases with the increase in ambient temperature, solar intensity, and evaporation temperature which is found to be the main factor that affects the thermal efficiency of the collector and can reach nearly 0.26 °C/W.
3) The experimental results suggest that the heat flux of the PHP absorber's evaporation section concentrated by CPC with a concentration ratio of 3.4 is appropriate and the use of CPC is reasonable.

4) The proposed design offers a promising efficiency of 50% when compared with conventional solar collectors and PHP solar collectors.

Acknowledgments

The work was financially supported by the National Natural Science Foundation of China (51506004), Beijing Natural Science Foundation (3162009), Scientific Research Project of Beijing Educational Committee (KM201410016001) and Research Fund of Beijing University of Civil Engineering and Architecture.

Nomenclature

A	area (m^2)
CR	concentration ratio of CPC
c	specific heat capacity (kJ/kg•K)
d	diameter (m)
D	aperture width (m)
H	height of CPC (mm)
m	mass flow rate (kg/s)
n	number of PHP turns
I	solar irradiation density (W/ m2)
ID	inner diameter (mm)
i	the number of a thermal couple
OD	outer diameter (mm)
Q	Heat transfer rate (W)
q	heat flux (W/m2)
T	temperature (°C)
R	thermal resistance (°C/W)

Greek symbols

η	efficiency of the solar collector
σ	surface tension of the working fluids (N/m)
ρ	density of the working fluids (kg/m^3)
φ	angle between the incident ray and the X-axis (°)
θ_A	aperture angle of the CPC (°)

Subscripts

1-13	location of thermal couples

c	condensation section
e	evaporation section
in	inlet of the hot water tank
l	liquid
r/rad	radial direction
out	outlet of the hot water tank
p	plate
s	solar energy
T	temperature
w	water
v	vapor

436
437
438
439 **References**

440 [1] Sabiha MA, Saidur R, Mekhilef S, Mahian O. Progress and latest developments of evacuated
441 tube solar collectors. Renewable and Sustainable Energy Reviews. 2015;51:1038-54.
442 [2] Muhammad MJ, Muhammad IA, Sidik NAC, Yazid MNAWM. Thermal performance
443 enhancement of flat-plate and evacuated tube solar collectors using nanofluid: A review. Int
444 Commun Heat Mass. 2016;76:6-15.
445 [3] Pandey KM, Chaurasiya R. A review on analysis and development of solar flat plate collector.
446 Renewable and Sustainable Energy Reviews. 2017;67:641-50.
447 [4] Verma SK, Tiwari AK, Chauhan DS. Experimental evaluation of flat plate solar collector using
448 nanofluids. Energ Convers Manage. 2017;134:103-15.
449 [5] Sabiha M, Saidur R, Hassani S, Said Z, Mekhilef S. Energy performance of an evacuated tube
450 solar collector using single walled carbon nanotubes nanofluids. Energ Convers Manage.

2015;105:1377-88.

[6] Mosleh HJ, Mamouri SJ, Shafii M, Sima AH. A new desalination system using a combination of heat pipe, evacuated tube and parabolic trough collector. Energ Convers Manage. 2015;99:141-50.

[7] Akachi H. Structure of a heat pipe. Google Patents; 1990.

[8] Miura M, Nagasaki T, Ito Y. Experimental investigation of heat transport with oscillating liquid column in pulsating heat pipe using forced oscillation system. Int J Heat Mass Tran. 2017;106:997-1004.

[9] Han X, Wang X, Zheng H, Xu X, Chen G. Review of the development of pulsating heat pipe for heat dissipation. Renewable and Sustainable Energy Reviews. 2016;59:692-709.

[10] Pastukhov V, Maydanik YF. Development of a pulsating heat pipe with a directional circulation of a working fluid. Appl Therm Eng. 2016;109:155-61.

[11] Khandekar S, Dollinger N, Groll M. Understanding operational regimes of closed loop pulsating heat pipes: an experimental study. Appl Therm Eng. 2003;23:707-19.

[12] Lee J, Kim SJ. Effect of channel geometry on the operating limit of micro pulsating heat pipes. Int J Heat Mass Tran. 2017;107:204-12.

[13] Jang DS, Lee JS, Ahn JH, Kim D, Kim Y. Flow patterns and heat transfer characteristics of flat plate pulsating heat pipes with various asymmetric and aspect ratios of the channels. Appl Therm Eng. 2017;114:211-20.

[14] Meena P, Rittidech S, Poomsa-Ad N. Application of closed-loop oscillating heat-pipe with check valves (CLOHP/CV) air-preheater for reduced relative-humidity in drying systems. Appl Energ. 2007;84:553-64.

[15] Samana T, Kiatsiriroat T, Nuntaphan A. Air-Side Performance Analysis of a Wire-on-Tube Heat Exchanger With an Oscillating Heat Pipe as an Extended Surface Under Natural Convection

474 Conditions. Heat Transfer Eng. 2012;33:1033-9.
475 [16] Nuntaphan A, Vithayasai S, Vorayos N, Vorayos N, Kiatsiriroat T. Use of oscillating heat pipe
476 technique as extended surface in wire-on-tube heat exchanger for heat transfer enhancement. Int
477 Commun Heat Mass. 2010;37:287-92.
478 [17] Burban G, Ayel V, Alexandre A, Lagonotte R, Bertin Y, Romestant C. Experimental
479 investigation of a pulsating heat pipe for hybrid vehicle applications. Appl Therm Eng.
480 2013;50:94-103.
481 [18] Naik R, Pinto L, Narasimha KR, Pundarika G. Theoretical Studies on the Application of
482 Pulsating Heat Pipe in Vapour Compression Refrigeration System. Appl Mech Mater.
483 2014;592-594:1801-6.
484 [19] Tang WW, Kou GX, Hu LL, Zhou HW, Feng B. On Application of Looped Pulsating Heat-Pipe
485 in High-Power LED for Street Light. Adv Mater Res-Switz. 2013;732-733:265-9.
486 [20] Chao CI, Lin WK, Hsiung TY, Liaw KC, Wang M, Yeh YC, et al. Performance Tests of
487 Defrosting Plates Designed with a Pulsating Heat Pipe (Php) as the Heat Carrier. J Enhanc Heat
488 Transf. 2013;20:527-41.
489 [21] Rittidech S, Wannapakne S. Experimental study of the performance of a solar collector by
490 closed-end oscillating heat pipe (CEOHP). Appl Therm Eng. 2007;27:1978-85.
491 [22] Nguyen KB, Yoon SH, Choi JH. Effect of working-fluid filling ratio and cooling-water flow
492 rate on the performance of solar collector with closed-loop oscillating heat pipe. J Mech Sci
493 Technol. 2012;26:251-8.
494 [23] Kargarsharifabad H, Mamouri SJ, Shafii MB, Rahni MT. Experimental investigation of the
495 effect of using closed-loop pulsating heat pipe on the performance of a flat plate solar collector. J
496 Renew Sustain Ener. 2013;5.

497 [24] Jalilian M, Kargarsharifabad H, Godarzi AA, Ghofrani A, Shafii M. Simulation and
498 optimization of pulsating heat pipe flat-plate solar collectors using neural networks and genetic
499 algorithm: a semi-experimental investigation. Clean Technologies and Environmental Policy.
500 2016;18:2251-64.
501 [25] Rittidech S, Donmaung A, Kumsombut K. Experimental study of the performance of a circular
502 tube solar collector with closed-loop oscillating heat-pipe with check valve (CLOHP/CV). Renew
503 Energ. 2009;34:2234-8.
504 [26] Yang YP, Xian HZ, Liu DY, Chen CB, Du XZ. Investigation on the Feasibility of
505 Oscillating-Flow Heat Pipe Applied in the Solar Collector. Int J Green Energy. 2009;6:426-36.
506 [27] Devanarayanan K, Kalidasa Murugavel K. Integrated collector storage solar water heater with
507 compound parabolic concentrator -development and progress. Renewable and Sustainable Energy
508 Reviews. 2014;39:51-64.
509 [28] Yoon SH, Oh C, Choi JH. A study on the heat transfer characteristics of a self-oscillating heat
510 pipe. Ksme Int J. 2002;16:354-62.
511 [29] Zhang XM, Xu JL, Zhou ZQ. Experimental study of a pulsating heat pipe using FC-72, ethanol,
512 and water as working fluids. Exp Heat Transfer. 2004;17:47-67.
513 [30] Borgmeyer B, Ma HB. Experimental investigation of oscillating motions in a flat plate
514 pulsating heat pipe. J Thermophys Heat Tr. 2007;21:405-9.
515 [31] Dmitrin VI, Maidanik YF. Experimental investigations of a closed-loop oscillating heat pipe.
516 High Temp. 2007;45:703-7.
517 [32] Yang H, Khandekar S, Groll M. Operational limit of closed loop pulsating heat pipes. Appl
518 Therm Eng. 2008;28:49-59.
519 [33] Sarangi RK, Rane MV. Experimental Investigations for Start Up and Maximum Heat Load of

520 Closed Loop Pulsating Heat Pipe. Procedia Engineer. 2013;51:683-7.
521 [34] Naik R, Varadarajan V, Pundarika G, Narasimha KR. Experimental Investigation and
522 Performance Evaluation of a Closed Loop Pulsating Heat Pipe. J Appl Fluid Mech. 2013;6:267-75.
523 [35] Mameli M, Marengo M, Khandekar S. Local heat transfer measurement and thermo-fluid
524 characterization of a pulsating heat pipe. Int J Therm Sci. 2014;75:140-52.
525 [36] Cui XY, Zhu Y, Li ZH, Shun SD. Combination study of operation characteristics and heat
526 transfer mechanism for pulsating heat pipe. Appl Therm Eng. 2014;65:394-402.
527 [37] Karthikeyan VK, Ramachandran K, Pillai BC, Solomon AB. Effect of nanofluids on thermal
528 performance of closed loop pulsating heat pipe. Exp Therm Fluid Sci. 2014;54:171-8.
529 [38] Hao TT, Ma XH, Lan Z, Li N, Zhao YZ. Effects of Superhydrophobic and Superhydrophilic
530 Surfaces on Heat Transfer and Oscillating Motion of an Oscillating Heat Pipe. J Heat Trans-T Asme.
531 2014;136.
532 [39] Mohammadi M, Mohammadi M, Ghahremani AR, Shafii MB, Mohammadi N. Experimental
533 Investigation of Thermal Resistance of a Ferrofluidic Closed-Loop Pulsating Heat Pipe. Heat
534 Transfer Eng. 2014;35:25-33.
535 [40] Karthikeyan VK, Khandekar S, Pillai BC, Sharma PK. Infrared thermography of a pulsating
536 heat pipe: Flow regimes and multiple steady states. Appl Therm Eng. 2014;62:470-80.
537 [41] Tseng CY, Yang KS, Chien KH, Jeng MS, Wang CC. Investigation of the performance of
538 pulsating heat pipe subject to uniform/alternating tube diameters. Exp Therm Fluid Sci.
539 2014;54:85-92.
540 [42] Mohammadi M, Taslimifar M, Haghayegh S, Hannani SK, Shafii MB, Saidi MH, et al.
541 Open-Loop Pulsating Heat Pipes Charged With Magnetic Nanofluids: Powerful Candidates for
542 Future Electronic Coolers. Nanosc Microsc Therm. 2014;18:18-38.

543 [43] Mameli M, Manno V, Filippeschi S, Marengo M. Thermal instability of a Closed Loop
544 Pulsating Heat Pipe: Combined effect of orientation and filling ratio. Exp Therm Fluid Sci.
545 2014;59:222-9.
546 [44] Xian HZ, Xu WJ, Zhang YN, Du XZ, Yang YP. Thermal characteristics and flow patterns of
547 oscillating heat pipe with pulse heating. Int J Heat Mass Tran. 2014;79:332-41.
548 [45] Pachghare PR, Mahalle AM. Thermo-hydrodynamics of closed loop pulsating heat pipe: an
549 experimental study. J Mech Sci Technol. 2014;28:3387-94.
550 [46] Xian HZ, Xu WJ, Zhang YN, Du XZ, Yang YP. Experimental investigations of dynamic fluid
551 flow in oscillating heat pipe under pulse heating. Appl Therm Eng. 2015;88:376-83.
552 [47] Beerepoot M, Tam C, Philibert C, Frankl P. Technology Roadmap Solar Heating and Cooling.
553 International Energy Agency (IEA): Paris, France. 2012.
554 [48] M. Hammad. Experimental study of the performance of a solar collector cooled by heat pipe.
555 Energ Convers Manage. 1995;36:197–203.
556